Energy 212 (2020) 118692

Contents lists available at ScienceDirect

Energy

journal homepage: www.elsevier.com/locate/energy

High-grade bio-oil produced from coconut shell: A comparative study of microwave reactor and core-shell catalyst

Xiaocui Wei, Xiangfei Xue, Liu Wu, Haozhe Yu, Jie Liang*, Yifei Sun

Beijing Key Laboratory of Bio-inspired Energy Materials and Devices, School of Space and Environment, Beihang University, Beijing, 102206, China

ARTICLE INFO

Article history:
Received 7 July 2020
Received in revised form
13 August 2020
Accepted 19 August 2020
Available online 24 August 2020

Keywords:
Bio-oil
Microwave-assisted pyrolysis
Catalytic pyrolysis
Zeolites
Coconut shell

ABSTRACT

The quality of bio-oil can be improved by conducting biomass pyrolysis either over a core-shell hierarchical zeolite catalyst or in a microwave reactor. However, there is a lack of comparative studies on the individual effects of each factor (*e.g.*, catalysts, reactors) on bio-oil production. In this regard, the catalytic pyrolysis of coconut shell in a fixed-bed reactor and in a microwave reactor using the conventional ZSM-5 and core-shell hierarchical ZSM-5@SBA-15 catalysts was evaluated. With an emphasize on the production of hydrocarbons and phenols, the comparative effect of the core-shell catalyst and microwave reactor was demonstrated. The core-shell catalyst had the dual effect of regulating the bio-oil yield and composition. Compared to conventional ZSM-5 (25) with a SiO_2/Al_2O_3 ratio of 25, the core-shell ZSM-5 (25)@SBA-15 not only increased the bio-oil yield by at least 40%, but also approximately doubled the production of hydrocarbons, irrespective of the reactor type. In contrast, the microwave reactor played a greater role in regulating the bio-oil composition. Irrespective of the catalyst used, the fixed-bed reactor tended to generate phenolic-rich bio-oil, while the microwave reactor sharply reduced the phenol selectivity by at least doubling that for aromatics.

1. Introduction

The ever-increasing energy demand and depletion of fossil fuel are forcing our society to search for alternative energy sources. As the only sustainable carbon source, lignocellulosic biomass has attracted worldwide attention because it is readily converted to renewable bio-oils that may partially replace fossil fuels [1,2]. Catalytic fast pyrolysis (CFP) is a promising conversion technique for this purpose [3,4]. Generally, biomass CFP is carried out in a pyrolysis reactor at a rapid heating rate (10–200 °C/s) at medium temperature (400–600 °C) [5,6]. In an inert atmosphere, the biomass is first devolatilized to oxygen-rich pyrolysis vapors, which subsequently diffuse into the catalyst bed and undergo a series of reactions that generate hydrocarbon fuels in the gasoline- or diesel-range. The reactors and catalysts both play a critical role during biomass CFP. On one hand, the reactor provides a multiphase environment, wherein rapid and efficient heat transfer facilitates the primary devolatilization of biomass feedstocks. On the other hand, the catalyst facilitates rapid entry and access of pyrolysis vapors to the active sites, wherein a range of catalytic reactions take place. Therefore, to improve the quality of biofuel, careful selection of the reactors and catalyst are required to enable large-scale exploitation of biomass CFP.

Various reactor types have been studied for biomass CFP. For instance, the micro-pyroprobe reactor offers the advantages of easy operation and rapid catalyst screening [4]. However, the low biomass loading limits efficient biomass/catalyst mixing and the as-prepared bio-oil is somewhat different from that in bench-scale experiments [7]. The laboratory-scale fixed-bed reactor facilitates study of the operating parameters, but the low mass and heat transfer rates also limit their large-scale application [8]. Fluidized bed reactors are of more industrial relevance. Nevertheless, the heat transfer properties, feedstock mixing conditions, and particle size requirements are dependent on specific reactors [9–11]. Recently, an innovative microwave reactor was developed, using microwave as the energy source. During biomass pyrolysis, the microwave penetrates the biomass, interacts with charged particles, and is converted to thermal energy throughout the biomass volume [12]. Therefore, the microwave reactor is advantageous for achieving uniform heating and overcomes the heat transfer limitation in conventional-heating reactors [13]. To enhance the absorption of microwaves by dry biomass, additional microwave

* Corresponding author.
E-mail address: jieliang@buaa.edu.cn (J. Liang).

https://doi.org/10.1016/j.energy.2020.118692
0360-5442/

absorbents are always used in the microwave reactor and fast pyrolysis can be achieved [14]. Microwave reactors have been widely applied in biomass pyrolysis [15,16]. For instance, the microwave-assisted pyrolysis (MAP) of cellulose yileds phenol-rich bio-oil [17]; the MAP of cigarette filters leads to an ester-rich bio-oil [18], and the microwave-assisted catalytic pyrolysis of soapstock or lignin produces a bio-oil abundant in aromatics, especially monocylic aromatic hydrocarbons (MAHs) [19,20]. Recently, a novel dual microwave system consisting of separate pyrolysis and catalyst beds was developed, which not only enhanced the production of hydrocarbons in the pyrolysis of woody oil, but also reduced the coke formation owing to the microplasma effect and hot spot phenomenon [21]. Therefore, microwave reactors are promising for improving the bio-oil quality by reducing the oxygen content.

Among the various deoxygenation catalysts, zeolites stand out owing to their unique porosity and abundant acid sites. The micropores of zeolites play a shape-selective role, while the distribution of acid sites determines the pyrolysis pathway of biomass [22,23]. Among the investigated zeolites, ZSM-5 exhibits unparalleled selectivity for gasoline-range hydrocarbons owing to its unique channel system and proper-acid characteristics. Nevertheless, the quality of the bio-oil produced with conventional ZSM-5 is still unsatisfactory due to the low bio-oil yield and high coke formation, which result from the small micropore size [24]. To solve this problem, hierarchical ZSM-5 has been synthesized and tested as a catalyst for biomass pyrolysis [25]. Recently, the application of core-shell micro-/mesoporous composite zeolites in the catalytic pyrolysis of biomass was also shown to be promising. In particular, the ZSM-5/MCM-41 composite zeolite afforded a higher hydrocarbon yield in the catalytic pyrolysis of various biomass feedstocks [20,26–28]. Another core-shell ZSM-5@SBA-15 catalyst also enhanced the content of hydrocarbons in bio-oil compared to that achieved by using only ZMS-5 in the pyrolysis of maize straw [29]. The remarkable catalytic effect was not only ascribed to the hierarchical porosity, which favored the diffusion of bulky molecules, but also to the silicon-rich exterior that inhibited the repolymerization of oxygenated intermediates to coke [30]. Therefore, core-shell hierarchical zeolites are also promising in the production of high-grade bio-oil with low oxygen content.

As aforementioned, both the microwave reactor and core-shell hierarchical zeolite catalyst can improve the quality of bio-oil. However, limited research on the comparative effect of catalysts and reactors on bio-oil production is available, which raises the question of which factor (*e.g.*, reactors, catalysts) is superior in enhancing the quality of bio-oil. Herein, the pyrolysis of coconut shell using the conventional and core-shell hierarchical ZSM-5 catalysts in a fixed-bed reactor and in a microwave reactor is evaluated. By focusing on the production of hydrocarbons and phenols, the specific contributions of the microwave reactor and core-shell catalyst on bio-oil production are demonstrated and compared.

2. Materials and methods

2.1. Biomass feedstocks

Coconut shell, collected from the north and south fruit markets in Hainan province, China, was used as the biomass feedstock. Before the pyrolysis experiments, the coconut shell was crushed and screened with a standard 40-mesh sieve to particle sizes less than 0.425 mm. These particles were then dried in an oven at 105 °C for 24 h to remove the moisture. Table 1 lists the characteristics of the coconut shell.

2.2. Synthesis of catalysts

Conventional ZSM-5 zeolites (Catalyst Plant of Nankai University) with SiO_2/Al_2O_3 ratios of 18, 25, and 46 were used as catalysts without additional treatment. The core-shell micro-/mesoporous ZSM-5 (25)@SBA-15 composite zeolite was synthesized as follows [31]. Under stirring, 3.56 g $MgSO_4{\cdot}7H_2O$ was added to a uniform solution containing 0.58 g triblock copolymer P123 ($M_w = 5800$) and 300 mL HCl (2 mol/L). Thereafter, 1.5 g ZSM-5 (25) powder was added and the mixture was sonicated for 30 min. Tetraethyl orthosilicate (1.5 g; TEOS, SiO_2 28.0 wt%) was then added dropwise, and after stirring for 24 h, the dispersion was transferred into an oven and heated at 100 °C for 24 h. The final sample was obtained after centrifugation, separation, and drying at 105 °C. The catalyst was calcined at 550 °C for 5 h prior to use in biomass pyrolysis.

2.3. Catalyst characterization

Powder X-ray diffraction (PXRD) patterns were obtained on a Bruker D8 Advance diffractometer with Cu-K_α radiation ($\lambda = 1.5406$ Å) at 40 kV and 20 mA. Data were aquuired in the 2θ range 0.6–6° at a scan rate of 1°/min, while that in the 2θ range 5–40° was collected at a step size of 8°/min. The sample morphologies were evaluated using a scanning electron microscope (SEM, ZEISS Sigma 500) at an accelerating voltage of 5 kV. Transition electron microscopy (TEM) images were recored on a JEM1200EX instrument at 200-kV accelerating voltage. N_2 adsorption-desorption experiments was measured at −196 °C on a Micromeritics ASAP 2100 instrument. From the isotherms, the specific surface area was calculated by the Brunauer-Emmett-Teller method; the micropore and mesopore volumes were distinguished by *t*-plot analysis. The pore size distribution in the conventional zeolites and core-shell zeolite composites were determined using the Horvath-Kawazoe (HK) model and nonlinear density functional theory (NLDFT), respectively. The acidity of the catalysts was studied by ammonia temperature-programmed desorption (NH_3-TPD) using on an AutoChem II 2920 apparatus. Infrared spectra with pyridine (Py) were recorded on a Nicolet IS10 Fourier–transform infrared (FT-IR) spectrometer. Before the experiment, the sample was first dehydrated under vacuum (10^{-5} Pa) at 300 °C for 6 h to eliminate the influence of adsorbed water molecules.

2.4. Experimental system and procedure

2.4.1. Fixed-bed pyrolysis experiment

As shown in Fig. 1, the fixed-bed pyrolysis apparatus comprised three sections: the pyrolysis system, carrier gas system, and condenser system. The middle of the pyrolysis reactor with a length of 950 mm and an inner diameter of 16 mm was filled with a mixture of 1.0 g of coconut shell and 1.0 g catalyst. Before pyrolysis, the apparatus was purged with N_2 gas at a flow of 200 mL/min for 30 min. The reactor was then heated to 500 °C under the action of electrically generated infrared light for 5 min, with a ramping rate of 10 °C/s. Meanwhile, the biomass vapor was purged by N_2 flow at a decreased rate of 100 mL/min, delivering it to a two-step cold trap (0 °C). After pyrolysis, the condensable liquid was collected, separated with dichloromethane, and weighed individually. The solid yield was determined from the solid residue left in the reactor. The gas yield was obtained by difference.

2.4.2. Microwave-assisted pyrolysis experiment

The microwave-assisted pyrolysis apparatus is depicted in Fig. 2. The microwave oven (CY-PY1100C-M) possesses a microwave heating area of 80 mm × 220 mm (diameter × width). A quartz tube was placed in this area and connected to the condensation

Table 1
Characteristics of coconut shell used in the experiments.

Chemical composition (wt%)		Proximate analysis (wt%)		Ultimate analysis (wt%)	
Cellulose	18.73	Volatiles	72.91	C	47.43
Hemicellulose	34.10	Moisture	4.36	H	5.12
Lignin	35.09	Ash	3.98	N	0.48
		Fixed carbon	18.75	O	37.20

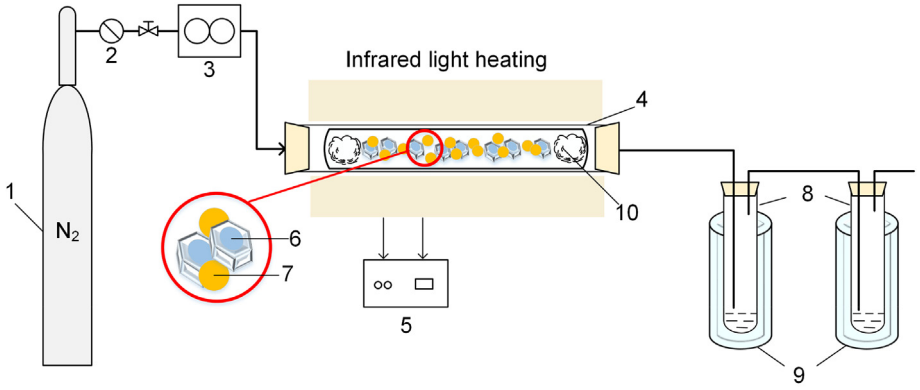

1, Nitrogen bottle; **2**, Gas valve; **3**, Mass flowmeter; **4**, Tube reactor; **5**, Controller; **6**, Catalysts; **7**, Biomass; **8**, Condenser; **9**, Cold trap; **10**, Quartz wool.

Fig. 1. Schematic diagram of fast pyrolysis apparatus.

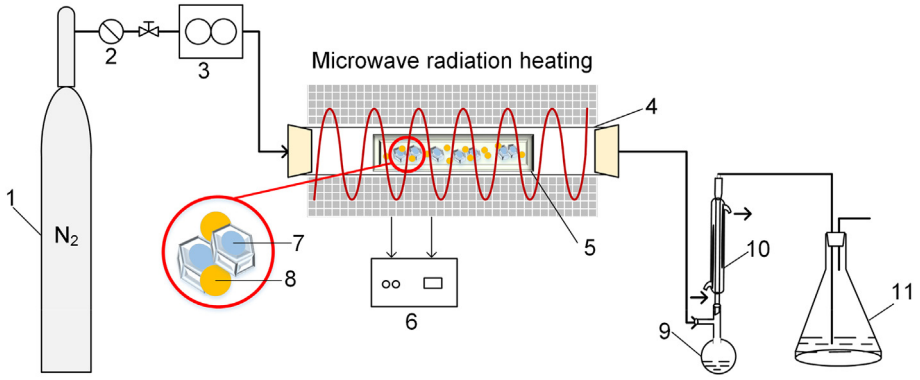

1, Nitrogen bottle; **2**, Gas valve; **3**, Mass flowmeter; **4**, Tube reactor; **5**, Quartz boat; **6**, Controller; **7**, Catalyst; **8**, Biomass; **9**, Oil collector; **10**, Condenser; **11**, Cold trap.

Fig. 2. Schematic diagram of microwave-assisted pyrolysis apparatus.

system by a stream outlet. A K-type thermocouple was inserted into the microwave oven for temperature control. After setting the temperatures, the microwave power is automatically regulated to the target; the maximum output power is 2.8 kW. Before pyrolysis, 10.0 g coconut shell and 10.0 g catalyst were thoroughly mixed and placed into a quartz boat, which was then placed in the middle of the microwave cavity. The pyrolysis condition is similar to that in fast pyrolysis experiment. That is, the apparatus was purged with N_2 gas flow (200 mL/min) for 30 min, and then the rate was reduced to 100 mL/min; the temperature of the microwave reactor was raised to 500 °C within 50 min and maintained for another 20 min. It should be pointed out that the low heating rate is caused by the instrument limit, and the utilized pyrolysis time was optimized from initial experiments to maximize the bio-oil yield. The pyrolysis vapors were driven out by N_2 gas flow and diffused into a bottom flask equipped with a condenser pipe and a secondary cold-trap loaded with dichloromethane. Similarly, the liquid collected in the condenser, consisting of oil and water phases, was separated and weighed individually. The solid yield was determined from the weight of solid left in the microwave reactor after pyrolysis. The gas yield was calculated by difference.

2.4.3. Bio-oil analysis

The bio-oil phase was further analyzed on a gas chromatograph-mass spectrometer (GC-MS, Shimadzu QP2020) equipped with a DB-5MS (30 m × 0.25 mm × 0.25 μm) capillary column. High-purity helium at a flow rate of 1.0 mL/min was used as the carrier gas. The GC program was set as follows: after maintaining the system at the initial temperature of 50 °C for 5 min, the GC temperature was increased to 200 °C at a ramping rate of 4 °C/min, and continuously to 280 °C within 7 min and held for another 5 min. Electron ionization (EI) combined with full scan mode is effective

for compound identification and was used in the experiments. The temperatures of the 0.5-μl injector and the ion source temperatures were set at 250 °C and 200 °C, respectively. Sample injection was performed in split injection mode with a split ratio of 10:1. The chemicals in bio-oil were identified by comparison with the mass spectra recorded in the National Institute of Standards and Technology (NIST 2014) library database. Their relative concentrations were determined from the area percentage (area%) of the chromatogram peaks (Fig. S1). Such a semiquantitative method has been proved facile for analyzing the bio-oil composition [32,33], given that hundreds of compounds may be present in bio-oil. In addition, because of the complexity of bio-oil, chemicals of the same functional group are grouped in evaluating the bio-oil quality.

3. Results and discussion

3.1. Catalyst characterization

Figure S2 presents the PXRD patterns of all the catalysts used in this study. For the traditional ZSM-5 series, the five sharp strong peaks located at $2\theta = 7.9°, 8.7°, 23.1°, 23.9°, 24.3°$ and the absence of humps in the 2θ range 20–25° confirmed the crystallinity and purity of ZSM-5 (18), ZSM-5 (25), and ZSM-5 (46). For the core-shell zeolite composite, the characteristic peaks of ZSM-5 were almost unchanged, suggesting that the structural integrity of the inner core was maintained after coating with the shell. The diffraction peak at $2\theta = 1°$ proved the existence of mesoporous SBA-15.

Although the PXRD patterns confirmed the co-existence of ZSM-5 and SBA-15 phases in the zeolite composite, the core-shell structure can only be verified by TEM analysis. Therefore, the TEM images were acquired. As shown in Fig. S3, the conventional ZSM-5 series displayed uniform phase contrast throughout the rectangle-shaped crystal. In contrast, the darker interior rectangle in ZSM-5@SBA-15 was surrounded by a lighter area, confirming the unique core-shell structure with a shell thickness of ~55 nm. This conclusion was further confirmed by the SEM images (Fig. S4). That is, the smooth external surfaces in conventional ZSM-5 became rough and sand-like in ZSM-5 (25)@SBA-15, owing to coating with the SBA-15 shell.

The porosity of these catalysts was further investigated by N_2 sorption experiments (Fig. 3). For all the traditional and core-shell ZSM-5 zeolites, a steep N_2 uptake was observed in the relative pressure (P/P_0) range below 0.001, confirming the presence of micropores. With increasing of relative pressure, the N_2 adsorption isotherm became saturated for the traditional ZSM-5 series. In contrast, the gas uptake increased continuously for the core-shell ZSM-5 (25)@SBA-15 and a hysteresis loop was observed in the relative pressure range of $0.45 < P/P_0 < 0.95$, confirming the presence of mesopores. Therefore, while the traditional ZSM-5 series exhibited only micropores (diameter: ~0.55 nm), ZSM-5 (25)@SBA-15 possessed a combined hierarchical micro-/mesoporous channel system (diameter: 0.55 nm and 6.8 nm). The textural properties of the catalysts are summarized in Table S1. With increasing Al content, the total surface area and volume of the ZSM-5 series first increased then decreased, and the maximum surface area and pore volume (411.7 m^2/g, 0.221 cm^3/g) was achieved by ZSM-5 (25) with a SiO_2/Al_2O_3 ratio of 25. The decreased values of ZSM-5 (18) can be explained by the presence of extra-framework Al that blocked the entrance of the micropores [34]. As expected, secondary coating of SBA-15 shell notably increased the total surface area and pore volume of the ZSM-5 (25) core to 458.3 m^2/g and 0.372 cm^3/g, respectively.

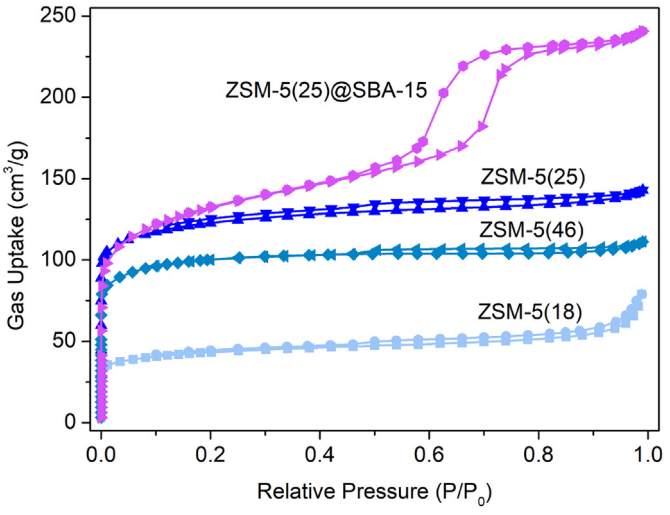

Fig. 3. N_2 adsorption–desorption isotherms for the catalysts.

The acidity of the different catalysts was studied by NH_3-TPD (Fig. S5). For both zeolite types, two temperature regions at 185–200 °C (weak acid sites) and 275–435 °C (strong acid sites) were observed in the NH_3-TPD curves. As shown in Table 2, the weak and strong acid sites both gradually increased with decreasing SiO_2/Al_2O_3 ratios of ZSM-5, and a double maximum (1.134 and 0.530 mmol/g) was achieved by ZSM-5 (18). The acidity of ZSM-5 (25)@SBA-15 was almost half that of ZSM-5 (25), despite the weak or strong acid sites. This suggested that coating of the mesoporous shell dramatically decreased the acidity of the ZSM-5 core.

To distinguish the acid sites in the zeolite catalysts, the IR spectra of pyridine (Py) was also measured (Fig. S6). All the catalysts exhibited bonds corresponding to Brønsted (~1545 cm^{-1}) and Lewis (~1450 cm^{-1}) acid sites bound pyridine [35]. At a lower desorption temperature of 200 °C, the Lewis acidity gradually increased with increasing of Al content in ZSM-5 (Table 3), whereas the Brønsted acidity first decreased then increased, where the minimum was achieved with ZSM-5 (25). This variation was more obvious at the higher desorption temperature of 400 °C. Nevertheless, the large Brønsted-to-Lewis (B/L) ratios (>1.2) indicate that a larger number of Brønsted acid sites are present in the ZSM-5 series. Compared to ZSM-5 (25), the ZSM-5 (25)@SBA-15 catalyst exhibited similar Brønsted and Lewis acidity at a desorption temperature of 400 °C, whereas the Lewis acidity was doubled at 200 °C and the resulting B/L ratio decreased by half to 0.7. Therefore, the core-shell ZSM-5 (25)@SBA-15 exhibited Lewis acid character at 200 °C, and a Brønsted acid character at higher temperature.

3.2. Pyrolysis experiments over conventional ZSM-5 catalysts

3.2.1. Fixed-bed pyrolysis of coconut shell

Fast pyrolysis of coconut shell was first conducted with the conventional ZSM-5 series. Fig. 4 presents the product distribution and bio-oil composition derived from non-catalytic and catalytic pyrolysis of coconut shell. As shown in Fig. 4a, non-catalytic pyrolysis of coconut shell yielded 38.5 wt% solids, 30.1 wt% gases, and 31.4 wt% liquids, which was further divided into 25.7 wt% water and 5.7 wt% bio-oil phases. Addition of the ZSM-5 (46) catalyst notably decreased the solid yield to 23.2 wt% while boosting the gas yield to 42.3 wt%. However, with increasing acidity of ZSM-5 (decrease in the SiO_2/Al_2O_3 ratio), the solid yield conversely increased to 29.9 wt % for ZSM-5 (18) and the gas yield linearly decreased to 37.0 wt%. This is because although acidic ZSM-5 promoted the cracking of biomass intermediates and inhibited their repolymerization to

Table 2
Acidity distribution of catalysts.

Catalysts	Peak 1 (T, °C)	Quantity (mmol/g)	Peak 2 (T, °C)	Quantity (mmol/g)	Total (mmol/g)
ZSM-5 (18)	199.2	1.134	434.9	0.530	1.664
ZSM-5 (25)	200.5	1.007	433.4	0.545	1.552
ZSM-5 (46)	189.2	0.565	409.5	0.499	1.064
ZSM-5 (25)@SBA-15	186.9	0.529	419.7	0.175	0.704

Table 3
The acid amount of catalysts evaluated by FT-IR of pyridine.

Catalysts	Desorption at 200 °C			Desorption at 400 °C		
	Brønsted	Lewis	B/L	Brønsted	Lewis	B/L
ZSM-5 (18)	256.27	209.60	1.22	227.40	127.91	1.78
ZSM-5 (25)	115.50	83.27	1.39	54.13	34.12	1.59
ZSM-5 (46)	135.27	37.59	3.60	110.02	14.66	7.50
ZSM-5 (25)@SBA-15	119.00	169.62	0.70	56.88	36.89	1.54

form coke, a more acidic catalyst would suffer from rapid deactivation by coke deposition [36]. The amount of liquid product increased with the addition of the ZSM-5 series and the largest bio-oil yield (13.5 wt%) was achieved with ZSM-5 (25), where the yield was twice that without catalysts. This once again confirmed that the acidic zeolites promoted the conversion of biomass intermediates into bio-oil products [37].

The complete chemical distribution of the bio-oil derived from fast pyrolysis of coconut shell with and without catalysts is listed in Tables S2–S3. For simplicity, the chemicals were classified into three groups: hydrocarbons, phenols, and oxygenated compounds (Fig. 4b). As expected, the bio-oil derived from non-catalytic pyrolysis was dominated by phenols (*e.g.*, phenol, methyl phenols, alkoxyl phenols) and oxygenated compounds (*e.g.*, furfural, benzofurans, 1H-Indenol) with almost no hydrocarbons. When acidic ZSM-5 (46) was used as the catalyst, the proportion of aromatic hydrocarbons (*e.g.*, naphthalene and its derivatives) started to increase, at the expense of the oxygen-containing compounds. This can be ascribed to the acid sites and shape-selective porosity of ZSM-5, which promote the deoxygenation and cracking of oxygenates into aromatics [25,38]. Although the proportion of phenols barely changed with the addition of ZSM-5 (46), the specific composition of the phenols was different from those obtained in the non-catalyzed reaction. For instance, the selectivity for methyl phenols decreased by 9.3 area%, while that for alkoxyl phenols increased by 10.6 area% (Fig. 4c). One reason is that the pathway for formation of methyl phenols competes with that for the formation of aromatics; that is, methyl phenols would be demethylated and aromatized to aromatics [8,39]. The other reason is that the introduction of ZSM-5 (46) would enhance the adsorption of alkoxyl phenols on the catalyst surface, thereby inhibiting the repolymerization of these alkoxy phenols to coke [40]. With increasing zeolite acidity, the production of aromatics and phenols were changed slightly, whereas the selectivity for other oxygenates continuously decreased to 10.9 area% for ZSM-5 (18), which is half of that for non-catalytic pyrolysis.

To better illustrate the catalytic effect of acidic ZSM-5 on bio-oil production, the absolute yield of value-added phenols and hydrocarbons is plotted as a function of the catalyst in Fig. 4d. As shown, all ZSM-5 catalysts enhanced the production of phenols and aromatics compared to that without a catalyst (0.04 wt% hydrocarbons, 4.4 wt% phenols). Nevertheless, phenols remained the major

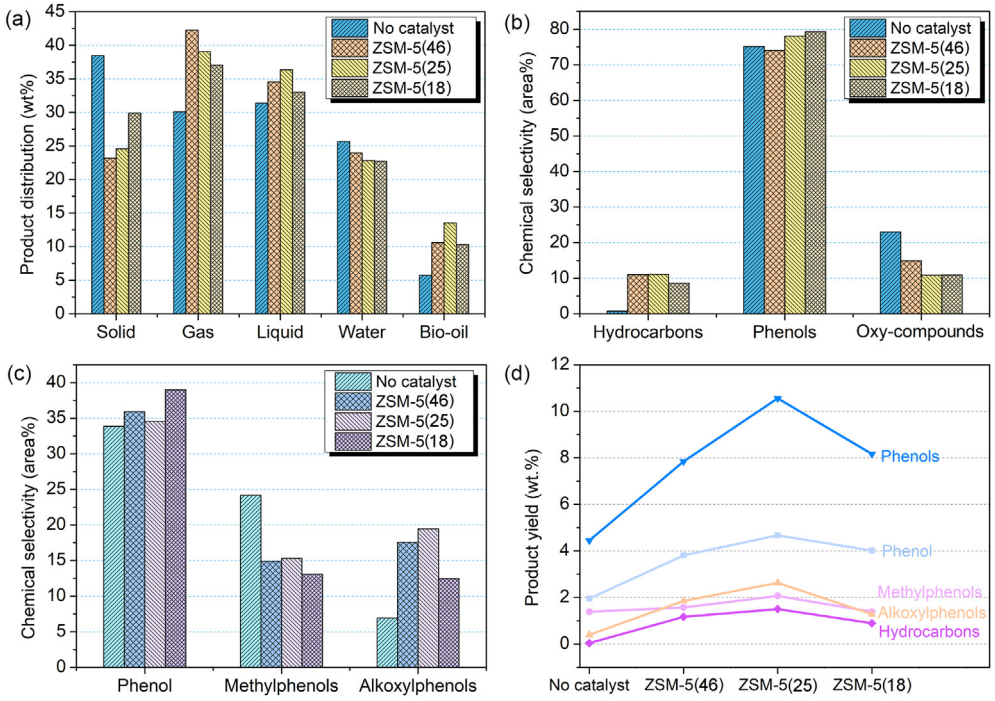

Fig. 4. Fast pyrolysis of coconut shell over ZSM-5 catalyst series. (a) Pyrolytic product yields; (b) bio-oil components; (c) selectivity for phenolic compounds; (d) absolute yields of phenols and hydrocarbons.

product in the bio-oil. This may be caused by the high energy of the C_{Ar}-OH bond, which is hard to break. Overall, ZSM-5 (25) with medium acidity afforded the a maximum hydrocarbon (1.5 wt%) and phenol (10.6 wt%) yield, despite the phenol type.

3.2.2. Microwave-assisted pyrolysis experiments

Fig. 5a presents the distribution of the products derived from microwave-assisted pyrolysis with and without the ZSM-5 catalysts. Compared to non-catalytic fast pyrolysis of coconut shell, microwave-assisted pyrolysis dramatically increased the gas yield from 30.1 wt% to 38.2 wt%, but decreased the liquid yield from 31.4 wt% to 21.2 wt%. The bio-oil fraction from microwave pyrolysis also decreased to below 1.8 wt%. This observation is consistent with previous reports that microwave heating promoted the secondary cracking of biomass vapors into permanent gases [14,41]. Addition of the ZSM-5 series notably increased the liquid yield at the expense of the solid yield. With increasing zeolite acidity, the liquid yield and bio-oil fraction first increased then decreased, where the maximum liquid and bio-oil yields of 30.9 wt%, 8.2 wt% were achieved with ZSM-5 (25) having a medium acidity. The solid yield followed the opposite trend. It was noted that the ZSM-5 (25) catalyst reduced the solid yield by half, which compensated for the increased production of gases to an extent. Therefore, it was suggested that the ZSM-5 catalysts also worked as microwave absorbents [42,43], which could conduct heat to the biomass and increase the heating rate. This is confirmed by the faster heating rate for ZSM-5 (25) than in the non-catalytic process (Fig. S7); ZSM-5 (25) with a medium Al loading functioned as the best microwave absorbent. The rapid heat conduction not only facilitated the devolatilization of biomass to primary vapors, but also maximized conversion of the vapors to bio-oil instead of to coke [6]. The higher temperature induced by ZSM-5 (25) also promoted secondary cracking of the biomass vapors to permanent gases and led to a higher gas yield [44].

The compounds in bio-oil obtained from microwave pyrolysis were also classified into hydrocarbons, phenols, and oxygenated compounds (Fig. 5b). The complete chemical list is presented in Tables S4–S5. Similar to fast pyrolysis without a catalyst, non-catalytic microwave pyrolysis also furnished bio-oil abundant in phenols (71.8 area%) and oxygenated species (27.2 area%), with almost no hydrocarbons (0.3 area%). Among the phenolic components (Fig. 5c), microwave pyrolysis sharply increased the proportion of alkoxyl phenols by 22.4 area%, but decreased the production of phenol and methyl phenols by 9.4 area% and 6.2 area%, respectively. Because the primary decomposition of lignin mainly yielded alkoxy phenols at low temperature (<475 °C), which were subsequently converted into phenol and alkyl phenols *via* demethoxylation at a high temperature [45,46], it was inferred that the actual temperature of coconut shell during non-catalytic microwave pyrolysis is lower than 475 °C. This may be due to poor absorption of the microwaves by dry lignocellulose [47]. This dilemma was largely alleviated by the ZSM-5 catalysts. With addition of the ZSM-5 catalysts, microwave pyrolysis effectively converted the phenols and oxygenated species into hydrocarbons. Compared to the reaction without any catalyst (Fig. 5b), the selectivity towards phenols was decreased by 15.6–19.5 area% with use of ZSM-5. Specifically, the selectivity for alkoxyl phenols was reduced by 4.1–11.5 area% owing to their transformation to phenol by removal of the alkoxyl groups (Fig. 5c). However, because the "demethoxylation of alkoxyl phenols to phenol" occurred simultaneously with "alkylation of phenol to methyl phenols" [46,48], the selectivity for intermediate phenols also decreased with addition of the ZSM-5 catalysts. The same is true for methyl phenols, which continuously diffuse into the zeolite channels and undergo a series of reactions such as cracking, deoxygenation, and aromatization before being converted to aromatic hydrocarbons. Notably, the most acidic ZSM-5 (18) exhibited the highest phenol selectivity. This may be caused by the predominant demethoxylation relative to the alkylation reaction, which led to more phenol prior to conversion to methyl phenols. In addition, the least acidic ZSM-5 (46) presented the lowest

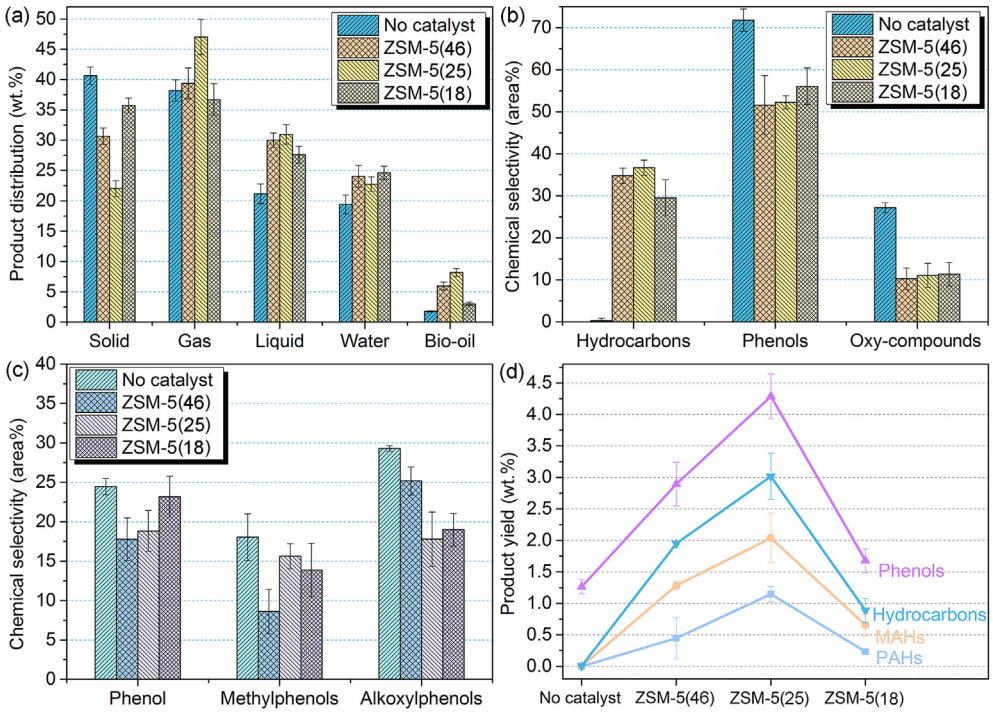

Fig. 5. Microwave-assisted pyrolysis of coconut shell over ZSM-5 catalyst series. (a) Pyrolytic product yields; (b) bio-oil components; (c) selectivity for phenolic compounds; (d) absolute yields of phenols and hydrocarbons.

selectivity for methyl phenol, as the aromatization reaction dominated the alkylation reaction. Therefore, an optimum zeolite acidity is required for the conversion of phenols into aromatics. ZSM-5 (25) afforded the highest hydrocarbon selectivity (36.7 area%) in microwave-assisted pyrolysis, where the selectivity is three times of that of fast pyrolysis (11.1 area%). The ZSM-5 (25) catalyst also yielded the largest fraction (14.0 area%) of monoaromatic hydrocarbons (MAHs), such as toluene, xylene, and mesitylene (Table S5). This confirmed the advantages of microwave heating in cracking the heavy bio-oil components [14].

The absolute yields of phenols and hydrocarbons are presented in Fig. 5d as a function of the ZSM-5 series. As indicated, all of the catalysts enhanced the production of phenols and hydrocarbons. With increasing zeolite acidity, the yield of phenols and hydrocarbons (*e.g.*, MAHs, PAHs) first increased then declined, where the maximum yields of all compounds were obtained with ZSM-5 (25). The maximum production of hydrocarbons (3.0 wt%) was higher than that obtained from fast pyrolysis over ZSM-5 (25). However, the maximum phenols yield (4.3 wt%) for microwave-assisted pyrolysis was much lower, owing to the low bio-oil yield and phenols selectivity of this process.

As mentioned above, ZSM-5 (25) with medium acidity afforded the maximum bio-oil yield and quality, irrespective of the use of a fixed-bed reactor or microwave reactor. Therefore, in the next section, the core-shell hierarchical counterpart of ZSM-5 (25), denoted as ZSM-5 (25)@SBA-15, is further tested as a catalyst in the pyrolysis of coconut shell, aiming to investigate the effect of the core-shell structure on bio-oil production.

3.3. Pyrolysis of coconut shell over core-shell ZSM-5(25)@SBA-15 catalyst

3.3.1. Fixed-bed pyrolysis experiment

Fig. 6a presents a comparison of the yield of pyrolytic products obtained over ZSM-5 (25) and ZSM-5 (25)@SBA-15 in the fixed-bed reactor. Similar to ZSM-5 (25), the addition of ZSM-5 (25)@SBA-15 increased the yield of gas and liquid at the expense of the solid yield. However, compared to ZSM-5 (25), ZSM-5 (25)@SBA-15 with a silica shell slightly reduced the production of gases, while increasing that of liquid. This is attributed to a longer residence time of the primary vapor within ZSM-5 (25)@SBA-15 and the reduced cracking ability of the core-shell hierarchical zeolite. The lowered cracking ability was further confirmed by the reduced water yield for ZSM-5 (25)@SBA-15, which consequently led to a higher bio-oil yield (19.3 wt%). It is noted that the bio-oil yield was not only 5.7 wt% larger than that obtained with ZSM-5 (25), but was also three times that derived from non-catalytic pyrolysis (5.7 wt%). This indicates that the core-shell ZSM-5 (25)@SBA-15 is more beneficial for bio-oil production.

The components of bio-oil produced over ZSM-5 (25)@SBA-15 were also classified into hydrocarbons, phenols, and oxygenated compounds (Fig. 6b). The complete compound distribution is listed in Table S6. Similar to the reaction over ZSM-5 (25), phenols were the predominant component when ZSM-5 (25)@SBA-15 was used as the catalyst. The phenols selectivity of both catalysts were similar, at ~78 area%. However, when the subgroups of phenols are considered (Fig. 6c), the ZSM-5 (25)@SBA-15 catalyst obviously decreased the alkoxyl phenols selectivity by 6.8 area%. This, plus the reduced selectivity for oxygenated compounds, suggests that the mesoporous channels in ZSM-5 (25)@SBA-15 allowed the entrance of more active species and enabled their deoxygenation to hydrocarbons (Fig. 6b). Therefore, the hydrocarbon selectivity (19.3 area%) achieved with ZSM-5 (25)@SBA-15 was almost twice that obtained with ZSM-5 (25) (11.1 area%). However, it should be noted that the hydrocarbons were still dominated by 2-ring aromatics, such as naphthalene and its derivatives (Table S6).

After combining the bio-oil yield, the ZSM-5 (25)@SBA-15 catalyst yielded 3.7 wt% hydrocarbons and 14.3 wt% phenols, including 6.3 wt% phenol, 2.9 wt% methyl phenols, and 2.4 wt% alkoxyl phenols (Fig. 6d). All the yields were higher than those

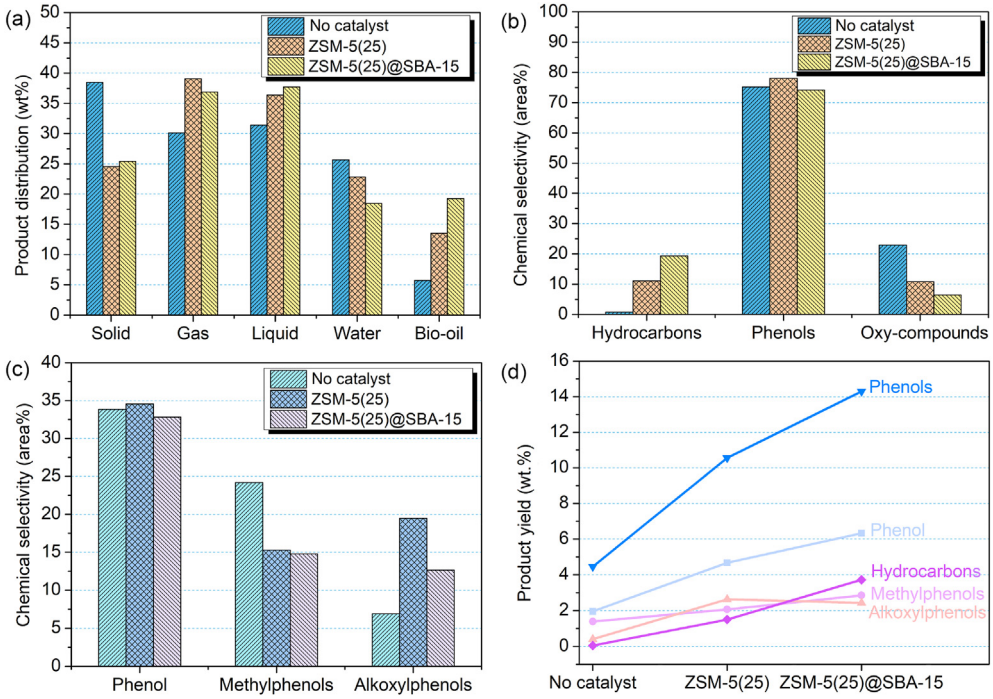

Fig. 6. Fast pyrolysis of coconut shell over ZSM-5 (25) and ZSM-5 (25)@SBA-15. (a) Pyrolytic product yields; (b) bio-oil components; (c) selectivity for phenolic compounds; (d) absolute yields of phenols and hydrocarbons.

obtained with ZSM-5 (25), with alkoxyl phenol as the only exception. This demonstrates that the core-shell hierarchical zeolite could improve the yield and quality of bio-oil in a fixed-bed reactor.

3.3.2. Microwave-assisted pyrolysis experiment

The core-shell ZSM-5 (25)@SBA-15 was later investigated as the catalyst in the microwave pyrolysis of coconut shell. As indicated, compared to the reaction without catalyst, the addition of acidic ZSM-5 (25)@SBA-15 considerably increased the liquid yield at the expense of the solid yield (Fig. 7a), and the bio-oil fraction increased dramatically by 13.8 wt%. This suggests that the ZSM-5 (25)@SBA-15 catalyst is also a good microwave absorbent, which facilitated heat conduction to the coconut shell and enhanced its conversion to bio-oil [14]. This is evidenced by the data in Fig. S7, wherein the core-shell zeolite also increased the heating rate in the initial 10 min in comparison to non-catalytic microwave pyrolysis. Compared to ZSM-5 (25), the less acidic ZSM-5 (25)@SBA-15 further reduced the yield of permanent gases and water, accompanied by doubling of the bio-oil yield and increased solid yield. This is attributed to the additional silicate shell in ZSM-5 (25)@SBA-15, which not only prolonged the residence time of biomass vapors within the catalyst, but also weakened the secondary cracking reactions [24]. A similar trend was observed for the reaction in the fixed-bed reactor, which suggests that the core-shell catalyst is more beneficial for bio-oil production, irrespective of the reactor type.

Fig. 7b presents the chemical components in the bio-oil fraction; the complete chemical distribution is listed in Table S7. Compared to non-catalytic microwave-assisted pyrolysis of coconut shell, the use of the ZSM-5 (25)@SBA-15 catalyst sharply increased the hydrocarbon selectivity from 0.3 area% to 41.7 area%, while decreasing that for phenols and oxygenates from 71.8 to 27.2 area% to 48.1 and 7.6 area%, respectively. Although this trend is similar to that of the reaction over ZSM-5 (25), the changes in the relative selectivity were larger for ZSM-5 (25)@SBA-15. This is attributed to the mesoporous channels in the SBA-15 shell, which helped to crack the bulky biomass intermediates into smaller molecules and facilitated their access to the acid sites inside the ZSM-5 channels. A similar result was obtained in the pyrolysis of biomass over ZSM-5/MCM-41 [26–28]. Regarding the subgroup of phenols (Fig. 7c), the lower selectivity of ZSM-5 (25)@SBA-15 for phenol and methyl phenols suggestes that the alkylation reaction outweighed the demeoxylation reaction, and more methyl phenols passed through the microporous channels and were converted into aromatics. Notably, the aromatics selectivity for ZSM-5 (25)@SBA-15 was 5.0 area% larger than that for ZSM-5 (25), where the major contribution is from MAHs (20.3 area% *vs.* 14.0 area%) (Tables S6–S7). This once again confirmed that the less acidic ZSM-5 (25)@SBA-15 enhances the secondary cracking of pyrolysis vapors, which promotes the cracking of heavy species in bio-oil into lighter molecules. Benefitting from the high bio-oil yield, the ZSM-5 (25)@SBA-15 catalyst further boosted the production of phenols (6.9 wt%), hydrocarbons (6.0 wt%), MAHs (2.9 wt%), and PAHs (3.1 wt%), the production of which was higher than that over ZSM-5 (25) (Fig. 7d). Therefore, ZSM-5 (25)@SBA-15 with a silicate mesoporous shell worked better in the microwave reactor, leading to a higher bio-oil yield and higher hydrocarbon selectivity in the bio-oil.

3.4. Comparison of contribution of microwave reactor and core-shell hierarchical zeolite catalyst to bio-oil production

As mentioned above, the reactors and catalysts both impact the pathway for pyrolysis of coconut shell, thereby affecting the bio-oil production. The microwave reactor plays a larger part in determining the bio-oil composition. In the infrared light-heated fixed-bed reactor, the non-catalytic pyrolysis of coconut shell leads to primary vapors mainly composed of oxygen-containing compounds (*e.g.*, phenols, furfural, benzofurans). Although the addition of catalysts promoted deoxygenation and cracking of the primary vapors to hydrocarbons, the resulting bio-oil was still dominated by

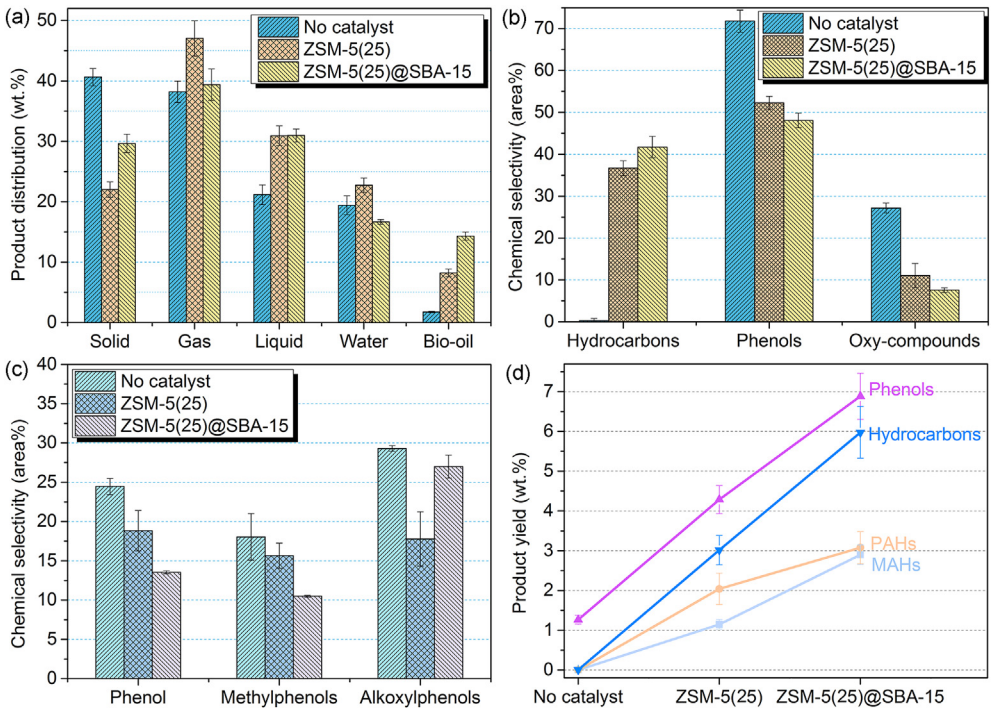

Fig. 7. Microwave-assisted pyrolysis of coconut shell over ZSM-5 (25) and ZSM-5 (25)@SBA-15. (a) Pyrolytic product yields; (b) bio-oil components; (c) selectivity for phenolic compounds; (d) absolute yields of phenols and hydrocarbons.

phenols, despite the use of ZSM-5 (25) or ZSM-5 (25)@SBA-15. This is because of the high bond energy of C_{Ar}–OH [49], and herein it is inferred that the conventional heating reactor could not provide enough energy to cleave the bonds in the phenols. In contrast, the microwave-heating reactor could decrease the activation energy of the cracking reactions and enable bond cleavage at lower temperature [50]. However, the bio-oil produced from non-catalytic microwave pyrolysis was still dominated by phenols. This is attributed to the poor ability of coconut shell to absorb microwaves, which results in a lower pyrolysis temperature, and the decomposition of lignin leads to more alkoxyl phenols [45,46,50]. As a good microwave absorbent [42,43], the added ZSM-5 (25) and ZSM-5 (25)@SBA-15 catalysts are conducive to heat conduction and transfer to the coconut shell, which favores cleavage of the C—C and C—O bonds in the biomass. The produced primary vapor could continuously diffuse into the catalyst bed and undergo deoxygenation, cracking, and aromatization reactions to yield aromatic hydrocarbons. Therefore, while the catalytic pyrolysis of coconut shell in the fixed-bed reactor leads to phenolic-rich bio-oil, the microwave-assisted catalytic pyrolysis notably increases the hydrocarbons in bio-oil. The core-shell hierarchical zeolite catalyst improves both the bio-oil yield and quality. Generally, the direct thermal decomposition of coconut shell yields primary vapors consisting mainly of oxygenated intermediates. After the primary vapors diffuse into the ZSM-5 (25) bed, the zeolite pores would stabilize the active intermediates (*e.g.*, alkoxy phenols, furfural) and inhibit their repolymerization to form coke, while the acid sites of the zeolite would deoxygenate the active intermediates to valuable components in bio-oil. The bio-oil yield is thereby boosted. The ZSM-5 (25)@SBA-15 catalyst with additional mesopores in the shell is conducive for cracking the bulky oxygenated intermediate into smaller molecules and facilities their access to the inner acid sites in ZSM-5 [26]. In addition, the less acidic ZSM-5 (25)@SBA-15 inhibited secondary cracking of the primary vapors to permanent gases by promoting their conversion to light components in bio-oil (*e.g.*, MAHs). Therefore, compared to ZSM-5 (25), the core-shell ZSM-5 (25)@SBA-15 catalyst could increase the bio-oil yield and production of MAHs, irrespective of the reactor type. As aforementioned, from the perspective of aromatics production, the microwave-assisted pyrolysis of coconut shell over the core-shell ZSM-5 (25)@SBA-15 catalyst is preferred. However, to produce phenolic-rich bio-oil, a combined fixed-bed reactor and core-shell zeolite is recommended.

4. Conclusions

Pyrolysis of coconut shell was conducted in a fixed-bed reactor or in a microwave reactor for bio-oil production, by using conventional ZSM-5 and core-shell hierarchical ZSM-5@SBA-15 as catalysts, respectively. The specific effects of the core-shell catalyst and microwave reactor were comparatively demonstrated. The core-shell hierarchical catalyst played a dual role in regulating the bio-oil yield and composition. Compared to conventional ZSM-5 (25), the core-shell ZSM-5 (25)@SBA-15 catalyst not only increased the bio-oil yield by 42—68%, but also increased the hydrocarbons yield by 146—200%, irrespective of the reactor type. In contrast, the microwave reactor contributed more to regulating the bio-oil composition. Irrespective of the catalyst used, the phenols selectivity achieved with the fixed-bed reactor was higher than 70 area%, whereas the microwave reactor enhanced the conversion of phenols to hydrocarbons (>36 area%). Therefore, the combination of the fixed-bed reactor and core-shell hierarchical ZSM-5@SBA-15 is recommended for producing phenolic-rich bio-oil (14.3 wt%), while the combination of the microwave reactor and ZSM-5@SBA-15 catalyst leads to a hydrocarbon-rich bio-oil (6 wt%). Although the results highlight the potential for high-grade hydrocarbon fuel production during microwave-assisted pyrolysis, efforts are still needed in promoting the large-scale use of microwaves for biomass valorization from the energy efficiency viewpoint.

Credit author statement

Xiaocui Wei: Conceptualization, Investigation, Writing-Original draft preparation, Xiangfei Xue: Data curation, Writing-Reviewing and Editing Liu Wu: Data curation, Writing-Reviewing and Editing Haozhe Yu: Writing-Reviewing and Editing, Jie Liang: Supervision Yifei Sun: Writing-Reviewing and Editing

Declaration of competing interest

The authors declare that they have no known competing financial interests or personal relationships that could have appeared to influence the work reported in this paper.

Acknowledgments

This work was supported by the National Natural Science Foundation of China (21906005); Beijing Natural Science Foundation (8194068); and PetroChina Innovation Foundation. Dr. J. Liang also acknowledges the financial support from Beihang University.

Appendix A. Supplementary data

Supplementary data to this article can be found online at https://doi.org/10.1016/j.energy.2020.118692.

References

[1] Ibarra-Gonzalez P, Rong BG. A review of the current state of biofuels production from lignocellulosic biomass using thermochemical conversion routes. Chin J Chem Eng 2019;27(7):1523—35.
[2] Jing Y, Guo Y, Xia Q, Liu X, Wang Y. Catalytic production of value-added chemicals and liquid fuels from lignocellulosic biomass. Inside Chem 2019;5(10):2520—46.
[3] Zhang Q, Chang J, Wang T, Xu Y. Review of biomass pyrolysis oil properties and upgrading research. Energy Convers Manag 2007;48(1):87—92.
[4] Mohan D, Pittman CU, Steele PH. Pyrolysis of wood/biomass for bio-oil: a critical review. Energy Fuels 2006;20:848—89.
[5] Bhoi PR, Ouedraogo AS, Soloiu V, Quirino R. Recent advances on catalysts for improving hydrocarbon compounds in bio-oil of biomass catalytic pyrolysis. Renew Sustain Energy Rev 2020;121:109676.
[6] Chen X, Che Q, Li S, Liu Z, Yang H, Chen Y, et al. Recent developments in lignocellulosic biomass catalytic fast pyrolysis: strategies for the optimization of bio-oil quality and yield. Fuel Process Technol 2019;196:106180.
[7] Wang K, Johnston PA, Brown RC. Comparison of in-situ and ex-situ catalytic pyrolysis in a micro-reactor system. Bioresour Technol 2014;173:124—31.
[8] Wang J, Zhong Z, Ding K, Li M, Hao N, Meng X, et al. Catalytic fast co-pyrolysis of bamboo sawdust and waste tire using a tandem reactor with cascade bubbling fluidized bed and fixed bed system. Energy Convers Manag 2019;180:60—71.
[9] Butler E, Devlin G, Meier D, McDonnell K. A review of recent laboratory research and commercial developments in fast pyrolysis and upgrading. Renew Sustain Energy Rev 2011;15(8):4171—86.
[10] Bridgwater AV. Review of fast pyrolysis of biomass and product upgrading. Biomass Bioenergy 2012;38:68—94.
[11] Cui H, Grace JR. Spouting of biomass particles: a review. Bioresour Technol 2008;99(10):4008—20.
[12] Fernandez BF. Microwave potential for bioenergy production. Renewable Energy Focus 2015;16:156—9.
[13] Morgan Jr HM, Bu Q, Liang J, Liu Y, Mao H, Shi A, et al. A review of catalytic microwave pyrolysis of lignocellulosic biomass for value-added fuel and chemicals. Bioresour Technol 2017;230:112—21.
[14] Borges FC, Du Z, Xie Q, Trierweiler JO, Cheng Y, Wan Y, et al. Fast microwave assisted pyrolysis of biomass using microwave absorbent. Bioresour Technol 2014;156:267—74.
[15] Beneroso D, Monti T, Kostas ET, Robinson J. Microwave pyrolysis of biomass for bio-oil production: scalable processing concepts. Chem Eng J 2017;316:481—98.
[16] State RN, Volceanov A, Muley P, Boldor D. A review of catalysts used in microwave assisted pyrolysis and gasification. Bioresour Technol 2019;277:179—94.

[17] Wang W, Wang M, Huang J, Tang N, Dang Z, Shi Y, et al. Microwave-assisted catalytic pyrolysis of cellulose for phenol-rich bio-oil production. J Energy Inst 2019;92(6):1997–2003.
[18] Wang W, Wang M, Huang J, Li X, Cai L, Shi SQ, et al. High efficiency pyrolysis of used cigarette filters for ester-rich bio-oil through microwave-assisted heating. J Clean Prod 2020;257:120596.
[19] Wang Y, Wu Q, Yang S, Yang Q, Wu J, Ma Z, et al. Microwave-assisted catalytic fast pyrolysis coupled with microwave-absorbent of soapstock for bio-oil in a downdraft reactor. Energy Convers Manag 2019;185:11–20.
[20] Zou R, Wang Y, Jiang L, Yu Z, Zhao Y, Wu Q, et al. Microwave-assisted co-pyrolysis of lignin and waste oil catalyzed by hierarchical ZSM-5/MCM-41 catalyst to produce aromatic hydrocarbons. Bioresour Technol 2019;289:121609.
[21] Yu Z, Jiang L, Wang Y, Li Y, Ke L, Yang Q, et al. Catalytic pyrolysis of woody oil over SiC foam-MCM-41 catalyst for aromatic-rich bio-oil production in a dual microwave system. J Clean Prod 2020;255:120179.
[22] Čejka J, Corma A, Zones S. Zeolites and catalysis: synthesis, reactions and applications, vol. 2. Weinheim: Wiley-VCH; 2010.
[23] Wang S, Cao B, Liu X, Xu L, Hu Y, Afonaa-Mensah S, et al. A comparative study on the quality of bio-oil derived from green macroalga Enteromorpha clathrata over metal modified ZSM-5 catalysts. Bioresour Technol 2018;256:446–55.
[24] Ibarra Á, Veloso A, Bilbao J, Arandes JM, Castaño P. Dual coke deactivation pathways during the catalytic cracking of raw bio-oil and vacuum gasoil in FCC conditions. Appl Catal, B 2016;182:336–46.
[25] Serrano DP, Melero JA, Morales G, Iglesias J, Pizarro P. Progress in the design of zeolite catalysts for biomass conversion into biofuels and bio-based chemicals. Catal Rev 2018;60(1):1–70.
[26] Li Z, Zhong Z, Zhang B, Gu J, Shi K. Catalytic fast pyrolysis of bamboo over micro-mesoporous composite molecular sieves. Energy Technol 2018;6(4):728–36.
[27] Zhang B, Zhang J, Zhong Z, Zhang Y, Song M, Wang X, et al. Conversion of poultry litter into bio-oil by microwave-assisted catalytic fast pyrolysis using microwave absorbent and hierarchical ZSM-5/MCM-41 catalyst. J Anal Appl Pyrolysis 2018;130:233–40.
[28] Zhang B, Zhong Z, Li T, Xue Z, Wang X, Ruan R. Biofuel production from distillers dried grains with solubles (DDGS) co-fed with waste agricultural plastic mulching films via microwave-assisted catalytic fast pyrolysis using microwave absorbent and hierarchical ZSM-5/MCM-41 catalyst. J Anal Appl Pyrolysis 2018;130:1–7.
[29] Xue X, Liu Y, Wu L, Pan X, Liang J, Sun Y. Catalytic fast pyrolysis of maize straw with a core-shell ZSM-5@SBA-15 catalyst for producing phenols and hydrocarbons. Bioresour Technol 2019;289:121691.
[30] Wang J, Zhong ZP, Song ZW, Ding K, Deng AD. Modification and regeneration of HZSM-5 catalyst in microwave assisted catalytic fast pyrolysis of mushroom waste. Energy Convers Manag 2016;123:29–34.
[31] Qian X, Du J, Li B, Si M, Yang Y, Hu Y, et al. Controllable fabrication of uniform core–shell structured zeolite@SBA-15 composites. Chem Sci 2011;2:2006–16.
[32] Ma W, Liu B, Zhang R, Gu T, Ji X, Zhong L, et al. Co-upgrading of raw bio-oil with kitchen waste oil through fluid catalytic cracking (FCC). Appl Energy 2018;217:233–40.
[33] Wang K, Dayton DC, Peters JE, Mante OD. Reactive catalytic fast pyrolysis of biomass to produce high-quality bio-crude. Green Chem 2017;19(14):3243–51.
[34] Verboekend D, Chabaneix AM, Thomas K, Gilson JP, Pérez-Ramírez J. Mesoporous ZSM-22 zeolite obtained by desilication: peculiarities associated with crystal morphology and aluminium distribution. CrystEngComm 2011;13:3408–16.
[35] Li M, Xing S, Yang L, Fu J, Lv P, Wang Z, et al. Nickel-loaded ZSM-5 catalysed hydrogenation of oleic acid: the game between acid sites and metal centres. Appl Catal A 2019;587:117112.
[36] Kelkar S, Saffron CM, Andreassi K, Li Z, Murkute A, Miller DJ, Pinnavaia TJ, Kriegel RM. A survey of catalysts for aromatics from fast pyrolysis of biomass. Appl Catal, B 2015;174–175:85–95.
[37] Rahman MM, Liu R, Cai J. Catalytic fast pyrolysis of biomass over zeolites for high quality bio-oil – a review. Fuel Process Technol 2018;180:32–46.
[38] Yuan C, Jiang D, Wang S, Barati B, Gong X, Cao B, et al. Study on catalytic pyrolysis mechanism of seaweed polysaccharide monomer. Combust Flame 2020;218:1–11.
[39] Martínez JD, Veses A, Mastral AM, Murillo R, Navarro MV, Puy N, et al. Co-pyrolysis of biomass with waste tyres: upgrading of liquid bio-fuel. Fuel Process Technol 2014;119:263–71.
[40] Ma Z, Troussard E, van Bokhoven JA. Controlling the selectivity to chemicals from lignin via catalytic fast pyrolysis. Appl Catal A 2012;423–424:130–6.
[41] Huang YF, Chiueh PT, Lo SL. A review on microwave pyrolysis of lignocellulosic biomass. Sustainable Environ Res 2016;26(3):103–9.
[42] Wei Z, Lin Z, Niu H, He H, Ji Y. Simultaneous desulfurization and denitrification by microwave reactor with ammonium bicarbonate and zeolite. J Hazard Mater 2009;162(2–3):837–41.
[43] Wei ZS, Du ZY, Lin ZH, He HM, Qiu RL. Removal of NOx by microwave reactor with ammonium bicarbonate and Ga-A zeolites at low temperature. Energy 2007;32(8):1455–9.
[44] Mohamed BA, Kim CS, Ellis N, Bi X. Microwave-assisted catalytic pyrolysis of switchgrass for improving bio-oil and biochar properties. Bioresour Technol 2016;201:121–32.
[45] Custodis VBF, Bährle C, Vogel F, van Bokhoven JA. Phenols and aromatics from fast pyrolysis of variously prepared lignins from hard- and softwoods. J Anal Appl Pyrolysis 2015;115:214–23.
[46] Kim YM, Jae J, Myung S, Sung BH, Dong JI, Park YK. Investigation into the lignin decomposition mechanism by analysis of the pyrolysis product of Pinus radiata. Bioresour Technol 2016;219:371–7.
[47] Krieger-Brockett B. Microwave pyrolysis of biomass. Research on chemical intermediates. Res Chem Intermed 1994;20(1):39–49.
[48] Wang J, Zhang B, Zhong Z, Ding K, Deng A, Min M, et al. Catalytic fast co-pyrolysis of bamboo residual and waste lubricating oil over an ex-situ dual catalytic beds of MgO and HZSM-5: analytical PY-GC/MS study. Energy Convers Manag 2017;139:222–31.
[49] Mullen CA, Boateng AA. Catalytic pyrolysis-GC/MS of lignin from several sources. Fuel Process Technol 2010;91(11):1446–58.
[50] Luo H, Bao L, Kong L, Sun Y. Low temperature microwave-assisted pyrolysis of wood sawdust for phenolic rich compounds: kinetics and dielectric properties analysis. Bioresour Technol 2017;238:109–15.